

# NJC

Accepted Manuscript



This is an *Accepted Manuscript*, which has been through the Royal Society of Chemistry peer review process and has been accepted for publication.

*Accepted Manuscripts* are published online shortly after acceptance, before technical editing, formatting and proof reading. Using this free service, authors can make their results available to the community, in citable form, before we publish the edited article. We will replace this *Accepted Manuscript* with the edited and formatted *Advance Article* as soon as it is available.

You can find more information about *Accepted Manuscripts* in the [Information for Authors](#).

Please note that technical editing may introduce minor changes to the text and/or graphics, which may alter content. The journal's standard [Terms & Conditions](#) and the [Ethical guidelines](#) still apply. In no event shall the Royal Society of Chemistry be held responsible for any errors or omissions in this *Accepted Manuscript* or any consequences arising from the use of any information it contains.



Journal Name

ARTICLE

## An arsenicniobate-based 3D framework with selective adsorption and anion-exchange properties

Received 00th January 20xx,  
Accepted 00th January 20xx

DOI: 10.1039/x0xx00000x

www.rsc.org/

Ning Li, Yiwei Liu, Ying Lu,\* Danfeng He, Shumei Liu, Xingquan Wang, Yangguang Li and Shuxia Liu\*

An arsenicniobate-based 3D porous framework,  $[\text{Cu}(\text{dap})_2]_4[\text{AsNb}_{12}\text{O}_{40}(\text{VO})_4] \cdot (\text{OH}) \cdot 7\text{H}_2\text{O}$  (**1**) (dap = 1,2-diaminopropane), was hydrothermally prepared and characterized by IR spectrum, elemental analysis, powder X-ray diffraction, thermogravimetric analysis and X-ray single-crystal diffraction. Structural analysis shows the framework is constructed by the tetra-vanadyl capped Keggin arsenicniobate  $[\text{AsNb}_{12}\text{O}_{40}(\text{VO})_4]^{7-}$  and four  $[\text{Cu}(\text{dap})_2]^{2+}$  linkers. The framework contains the 1D quadrangular channels of  $5.7 \times 5.7 \text{ \AA}$  along the crystallographic *c* axis. The overall framework is cationic and  $\text{OH}^-$  anions reside in the channels of framework for charge balance. Considering such a structural feature, we concentrated on the probability of the framework for selective adsorption and anion-exchange. The adsorption properties show **1** can selectively adsorb water molecules over ethanol to make them separate. Besides, anion-exchange studies for **1** suggest that the  $\text{OH}^-$  anions in the channels can be quantitatively exchanged by  $\text{SCN}^-$  anions.

### Introduction

Polyoxometalates (POMs) are an outstanding class of inorganic metal oxide clusters with structural diversity and versatile physical and chemical properties, they have potential applications in catalysis, magnetism, adsorption and biomedicine.<sup>1,2</sup> Polyoxoniobates (PONs) as a prominent branch of POMs are relatively less investigated due to the difficulty in synthesis controlling and the narrow working pH range compared with other traditional POMs.<sup>3,4</sup> Currently, increasing attention has been paid to PONs, and a number of isopolyoxoniobates (IPONs) clusters  $\{\text{Nb}_6\}$ ,  $\{\text{Nb}_{10}\}$ ,  $\{\text{Nb}_{20}\}$ ,  $\{\text{Nb}_{24}\}$ ,  $\{\text{Nb}_{27}\}$ ,  $\{\text{Nb}_{31}\}$ ,  $\{\text{Nb}_{32}\}$  and a series of transition-metal (TM)-containing IPONs were reported.<sup>5-9</sup> In contrast, heteropolyoxoniobates (HPONs) were much less reported. In 2002, the first classic Keggin-type HPON  $\{[\text{Ti}_2\text{O}_2][\text{SiNb}_{12}\text{O}_{40}]\}^{12-}$  was successfully synthesized.<sup>10</sup> Subsequently, several Keggin-type HPONs and their derivatives were prepared, namely,  $[\text{TNb}_{12}\text{O}_{40}]^{16-}$  (T = Si, Ge),  $[\text{Nb}_2\text{O}_2][\text{TNb}_{12}\text{O}_{40}]^{10-}$  (T = Si, Ge),  $[\text{T}_2(\text{TOH})_2\text{Nb}_{16}\text{O}_{54}]^{14-}$  (T = Si, Ge),  $[\text{TNb}_{18}\text{O}_{54}]^{n-}$  (T = Si, Ga and Al),  $[\text{GeNb}_{12}\text{O}_{40}(\text{NbO})]^{13-}$ ,  $[\text{TNb}_{12}\text{O}_{40}(\text{VO})_2]^{n-}$  (T = Ge, P and V),  $[\text{TNb}_8\text{V}_4\text{O}_{40}(\text{VO})_4]^{11-}$  (T = P, V),  $[\text{PNb}_{12}\text{O}_{40}(\text{VO})_6]^{3-}$  and  $[\text{VNb}_{12}\text{O}_{40}(\text{NbONO}_3)_2]^{11-}$ .<sup>11-19</sup> Till now, most of HPONs are based on P-, Si-, Ge- and V-centered polyanions, the construction of arsenic-centered polyoxoniobates is still very rare.<sup>20,21</sup> As is well known, vanadium and niobium are in the

same group and possess chemical similarity, thus, vanadium is a good candidate for the construction of Nb/V hybrids. Furthermore, we also expect that the transition-metal complexes (TMCs) as bridges are further introduced into HPONs to make the target compound porous, which may render HPONs-based framework additional functions such as adsorption and ion-exchange.

On the basis of the above points, we chose  $\text{K}_7\text{HfNb}_6\text{O}_{19} \cdot 13\text{H}_2\text{O}$  to react with  $\text{NaVO}_3$ ,  $\text{NaAsO}_2$ ,  $\text{Cu}(\text{OAc})_2 \cdot 2\text{H}_2\text{O}$  and dap (dap = 1,2-diaminopropane) under hydrothermal conditions, yielding an arsenicniobate-based 3D framework  $[\text{Cu}(\text{dap})_2]_4[\text{AsNb}_{12}\text{O}_{40}(\text{VO})_4] \cdot (\text{OH}) \cdot 7\text{H}_2\text{O}$  (**1**). Notably, the construction of arsenicniobates-based 3D frameworks is the first time in niobate chemistry. **1** shows high adsorption selectivity of water and ethanol, and effective removal of toxic  $\text{SCN}^-$  anions in aqueous solution.

### Experimental

#### Materials and methods

All chemicals were obtained commercially and used without further purification. The  $\text{K}_7\text{HfNb}_6\text{O}_{19} \cdot 13\text{H}_2\text{O}$  precursor was synthesized according to the procedure described in the literature and characterized by IR spectrum.<sup>22</sup> Elemental analyses for C, N and H were performed on a Perkin-Elmer 2400 CHN elemental analyzer, and for As, Nb, V, Cu were determined with a PLASMASPEC (I) ICP atomic emission spectrometer and for S was performed on a EuroVector EA3000 elemental analyzer. Powder X-ray diffraction (PXRD) measurements were performed on a Rigaku D/MAX-3 instrument with Cu-K $\alpha$  ( $\lambda = 1.5418 \text{ \AA}$ ) radiation at 293 K. The IR

Key Laboratory of Polyoxometalate Science of the Ministry of Education, College of Chemistry, Northeast Normal University, Changchun, Jilin 130024, China.

E-mail: liusx@nenu.edu.cn Fax: +86-431-85099328

Electronic Supplementary Information (ESI) available: IR spectra, PXRD patterns, TG curves and additional structural figures. See DOI: 10.1039/x0xx00000x

spectrum in KBr pellets were recorded in the range of 4000-400 $\text{cm}^{-1}$  with an Alpha Centaur FT-IR spectrophotometer. Thermogravimetric analyses (TGA) were performed on a Perkin-Elmer TGA7 instrument, with a heating rate of 10 $^{\circ}\text{C}/\text{min}$  under a nitrogen atmosphere. Gas adsorption measurements were carried out with a Hiden Isochema Intelligent Gravimetric Analyser (IGA-100B).

### Synthesis of compound 1

A mixture of  $\text{K}_7\text{HNb}_6\text{O}_{19}\cdot 13\text{H}_2\text{O}$  (0.10 g, 0.072 mmol),  $\text{NaVO}_3$  (0.05 g, 0.409 mmol),  $\text{NaAsO}_2$  (0.01g, 0.077 mmol) were added to 10 mL distilled water with stirring. Solid  $\text{Cu}(\text{OAc})_2\cdot 2\text{H}_2\text{O}$  (0.04 g, 0.18 mmol) was added in a single step, followed by the immediate addition of dap (0.02 mL). Then, the mixture was adjusted to pH 10.0 using 1 M KOH solution and transferred to a 23 mL Teflon-lined stainless steel autoclave. The Teflon-lined stainless steel autoclave was heated at 150  $^{\circ}\text{C}$  for 4 days and then cooled to room temperature at a rate of 10  $^{\circ}\text{C}/\text{h}$ . Brown block-like crystals were obtained by filtration, which were washed with distilled water and air-dried. Yield: 33.2% (based on Nb). Anal. Calcd (%) for 1: C 9.32, N 7.25, Cu 8.29, V 6.60, Nb 36.10. Found (%): C 9.52, N 7.18, Cu 8.18, V 6.96, Nb 35.72.

### X-Ray crystallography

The crystallographic data of 1 was conducted on a Bruker Smart Apex CCD diffractometer with Mo-K $\alpha$  monochromated radiation ( $\lambda = 0.71073 \text{ \AA}$ ) at room temperature. The linear absorption coefficients, scattering factors for the atoms, and anomalous dispersion corrections were taken from the International Tables for X-Ray Crystallography.<sup>23</sup> The structure was solved by the direct method and refined by the Full-matrix least-squares on  $F^2$  using SHELXS-97 crystallographic software package.<sup>24</sup> In the process of refinement, all non-H-atoms were refined with anisotropic displacement parameters. The H-atoms of the water molecules were not located and just put into the final molecular formula. H-atoms of the disordered dap were fixed in the calculated positions. The numbers of crystallization water molecules and hydroxyl groups were verified by X-ray structure and thermogravimetry analysis. The disorderd dap molecule and {VO} groups were explained in the the Supplementary Information (Fig. S6, S7). The good accordance between the experimental and simulated powder

**Table 1.** Crystal data and structural refinement for compounds 1.

| Compound                       | 1   |
|--------------------------------|---|
| Formula                        | $\text{C}_{24}\text{H}_{95}\text{N}_{16}\text{O}_{52}\text{AsCu}_4\text{Nb}_{12}\text{V}_4$ |
| M, g/mol                       | 3087.91   |
| Cryst. syst.                   | Tetragonal  |
| Space group                    | $I4/m$  |
| a, $\text{\AA}$                | 15.295(5)   |
| b, $\text{\AA}$                | 15.295(5)   |
| c, $\text{\AA}$                | 19.430(5)   |
| $\alpha$ , deg                 | 90  |
| $\beta$ , deg                  | 90  |
| $\gamma$ , deg                 | 90  |
| Vol, $\text{\AA}^3$            | 4545(3)   |
| Crystal size, $\text{mm}^3$    | $0.21 \times 0.18 \times 0.13$  |
| Z                              | 2   |
| Dcalc, $\text{mg}/\text{m}^3$  | 2.245   |
| Abs coeff, $\text{mm}^{-1}$    | 3.205   |
| Theta range, deg               | 1.69-25.00  |
| Reflns collected               | 12950   |
| F(000)                         | 2970  |
| R(int)                         | 0.0316  |
| GOF on $F^2$                   | 1.051   |
| $R_1 [I > 2\sigma(I)]^a$       | 0.0544  |
| $wR_2$ (all data) <sup>b</sup> | 0.1956  |

<sup>a</sup> $R_1 = \sum ||F_o| - |F_c|| / \sum |F_o|$ ; <sup>b</sup> $wR_2 = \{ \sum [w(F_o^2 - F_c^2)^2] / \sum [w(F_o^2)] \}^{1/2}$ .

XRD patterns suggests the phase purity (Fig. S2). The crystal data and structure refinement results are summarized in Table 1. CCDC-1407928 for 1 contains the supplementary crystallographic data for this paper. This data can be obtained free of charge from the Cambridge Crystallographic Data Centre.

## Results and discussion

### Synthesis and Structure

Compound 1 was synthesized under hydrothermal conditions using  $\text{K}_7\text{HNb}_6\text{O}_{19}\cdot 13\text{H}_2\text{O}$  as the precursor to react with  $\text{NaVO}_3$ ,  $\text{NaAsO}_2$ ,  $\text{Cu}(\text{OAc})_2\cdot 2\text{H}_2\text{O}$  and dap at pH 10.0 adjusted by 1 M KOH solution. Notably, the crystallinity of 1 was highly sensitive to the pH value of the reaction system, which was controlled in the range of 10.0 to 10.5, and no crystalline solid of 1 could be obtained outside this pH range. Additionally,

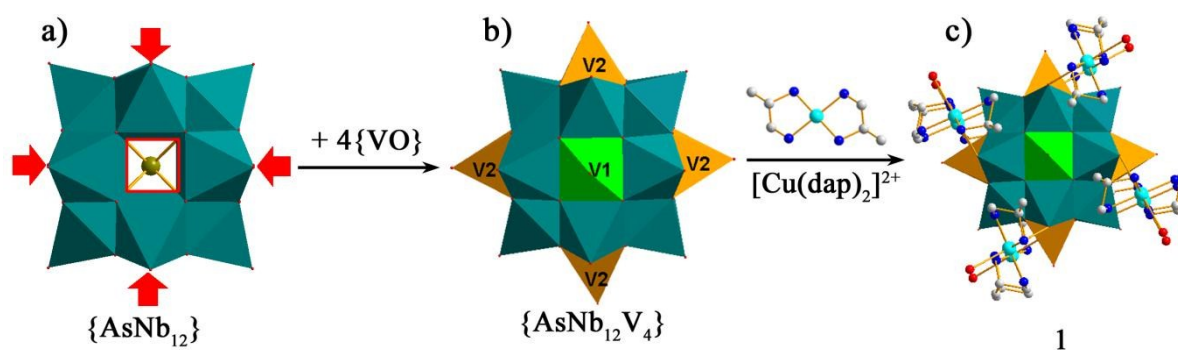


**Fig. 1.** Structural schematic diagram of 1 and  $\{\text{AsNb}_{12}\text{V}_4\}$  cluster (six quadrangles of  $\{\text{AsNb}_{12}\}$  are marked in red arrows and hollow box; color code:  $\text{NbO}_6$ , teal polyhedron;  $\text{V}(1)\text{O}_5$ , green polyhedron;  $\text{V}(2)\text{O}_5$ , orange polyhedron; As, dark yellow spheres; Cu, turquoise spheres; O, red spheres; C, grey spheres; N, blue spheres).

dap plays important roles, not only acting as reducing agent ( $V^V \rightarrow V^{IV}$ ) but also coordinating to  $Cu^{2+}$  ions for building extended structure. Structure analysis shows that **1** is a 3D porous framework constructed from  $[AsNb_{12}O_{40}(VO)_4]^{7-}$  ( $\{AsNb_{12}V_4\}$ ) clusters and  $[Cu(dap)_2]^{2+}$  linkers (Fig. 1c, 2). The  $\{AsNb_{12}V_4\}$  (Fig. 1b) is a tetra-vanadyl capped Keggin cluster constructed from one arsenic-centered  $\alpha$ -Keggin  $[AsNb_{12}O_{40}]^{15-}$  ( $\{AsNb_{12}\}$ ) anion and four terminal  $VO^{2+}$  groups. The  $\{AsNb_{12}V_4\}$  cluster was never reported before. As shown in Fig. 1, there are six quadrangles on the surface of  $\{AsNb_{12}\}$ , two  $\{V(1)O\}$  groups fully cap on two anteroposterior quadrangles of  $\{AsNb_{12}\}$ , whereas four V2 sites are found to be half-occupancy disordered together with terminal O6 sites, which means that each  $\{V(2)O\}$  group just possesses 50% opportunity over the remaining four opposite quadrangles. So, a total of four  $\{VO\}$  groups are given per cluster (containing V1 and V2). The detailed description of the disordered models can be seen in Fig. S6. Each  $V^{4+}$  ion is penta-coordinated by four  $\mu_2$ -O atoms from  $\{AsNb_{12}\}$  and one terminal O atom from  $VO^{2+}$  group. Bond-valence sum (BVS) calculations show all the V atoms are +4 oxidation state (Table S1), which is common in capped HPONs,<sup>16-18</sup> while the oxidation states of Nb, As and Cu atoms are +5, +5 and +2, respectively.

Moreover, each tetra-capped Keggin  $\{AsNb_{12}V_4\}$  cluster is connected by eight  $[Cu(dap)_2]^{2+}$  linkers via the terminal O atoms to form the 3D cationic  $\{[Cu(dap)_2]_4[AsNb_{12}O_{40}(VO)_4]\}^+$  framework (Fig. 2). Alternatively, the  $\{AsNb_{12}V_4\}$  cluster can be regarded as an eight-connected node to connect with eight other neighboring units via Nb–O–Cu–O–Nb bridges, generating the 3D porous framework. The most fascinating structural feature of the framework is that there exist 1D quadrangular channels of  $5.7 \times 5.7 \text{ \AA}$  along the crystallographic *c* axis (Fig. S1), in which  $H_2O$  molecules and  $OH^-$  anions are located. Charge calculation confirms that the overall framework is cationic and the  $OH^-$  anions residing in the channels are for charge balance. Furthermore, void-space

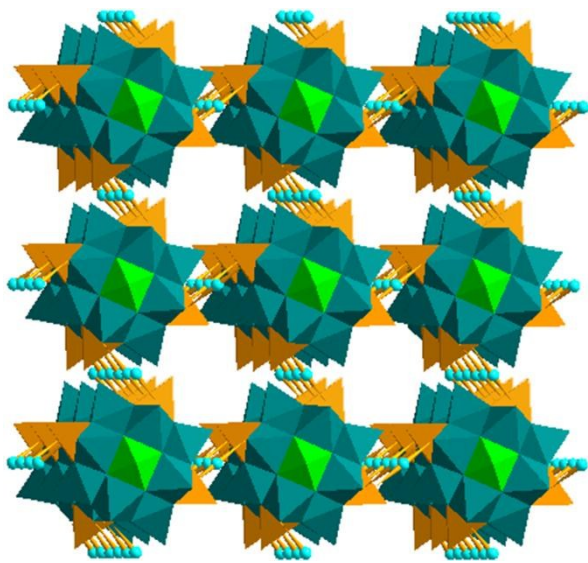


Fig. 2. View of the 3D porous framework of **1**, the dap ligands are omitted for clarity.

analysis using the program PLATON<sup>25</sup> indicates that the “solvent-accessible” space occupies 28.3% of the unit-cell volume ( $1286.2 \text{ \AA}^3$  out of  $4545.0 \text{ \AA}^3$ ). To our knowledge, **1** represents the first arsenoniobates-based 3D framework and also a rare 3D structure built by capped HPONs.<sup>18</sup> Each  $Cu^{2+}$  ion is hexa-coordinated by four N atoms from two dap molecules and two terminal O atoms from two  $\{AsNb_{12}V_4\}$  clusters. The average Cu–O and Cu–N bond length are 2.624 and 2.005  $\text{\AA}$ , respectively.

### IR Spectrum and TGA analyses

The IR spectrum of **1** was studied between 4000 and  $400 \text{ cm}^{-1}$  with a KBr pellet, which exhibits the characteristic vibration patterns resulting from the capped Keggin structure in the region of  $1100\text{--}400 \text{ cm}^{-1}$  (Fig. S3). There are three types of O atoms in the structure:  $O_t$  (terminal O atoms),  $O_b$  (bridging O atoms) and  $O_c$  (central O atoms). The terminal  $M = O_t$  ( $M = Nb/V$ ) vibrations appear at 936 and  $883 \text{ cm}^{-1}$ . The characteristic peaks at 696, 629 and  $497 \text{ cm}^{-1}$  are assigned to the bridging  $M\text{--}O_b\text{--}M$  vibrations. Band at  $1055 \text{ cm}^{-1}$  is attributed to  $As\text{--}O_c$  vibration.<sup>26</sup> The characteristic absorption bands of organic groups occur at  $1588\text{--}1169 \text{ cm}^{-1}$ . The broadened band centered at  $3239 \text{ cm}^{-1}$  is indicative of the O–H vibrations of the hydroxyl groups and water molecules. The thermal stability of **1** was investigated under a  $N_2$  atmosphere with a heating rate of  $10 \text{ }^\circ\text{C}/\text{min}$ . The TG curve shows three continuous weight losses steps in the range of  $30\text{--}800 \text{ }^\circ\text{C}$  (Fig. S4). The first weight loss is 5.18% (calc. 4.73%) from 30 to  $240 \text{ }^\circ\text{C}$ , assigned to the release of seven lattice water molecules and one hydroxyl group. The other two weight losses of 19.87% (calc. 19.73%) from 240 to  $618 \text{ }^\circ\text{C}$  correspond to the decomposition of eight dap molecules.

### Adsorption Properties

As mentioned above, **1** is a microporous framework with open channels. Therefore, it is expected that pores in **1** are accessible for small molecules. The sample was placed in a high vacuum oven at  $120 \text{ }^\circ\text{C}$  for 12 h to remove the guest solvent molecules before the measurements. We measured the adsorption isotherms of water and ethanol at 298 K. As shown in Fig. 3, the amount of water sorption increased with increasing pressure and was almost leveled off (ca.  $30.22 \text{ mg g}^{-1}$ ) around  $P/P_0 = 0.8$ , which is equivalent to the adsorption of 5.2  $H_2O$  molecules per formula unit. In contrast, the amounts of ethanol sorption ( $1.25 \text{ mg g}^{-1}$  at  $P/P_0 = 0.8$ ) was close to the surface adsorption and was negligible. The noninclusion of ethanol can be correlated to larger size of the ethanol compared with water. As we all know, water and ethanol are easy to form azeotrope and difficult to separate. The adsorption isotherms indicate that **1** can selectively adsorb water molecules over ethanol to make them separate. Therefore, the above adsorption studies suggest **1** will be a promising material for industrial alcohol purification.

Additionally, the adsorption studies for methanol and propanol were also carried out at 298 K. The sorption amounts of methanol and propanol were almost the same with that of ethanol, which were also negligible compared with that of water (Fig. S5).

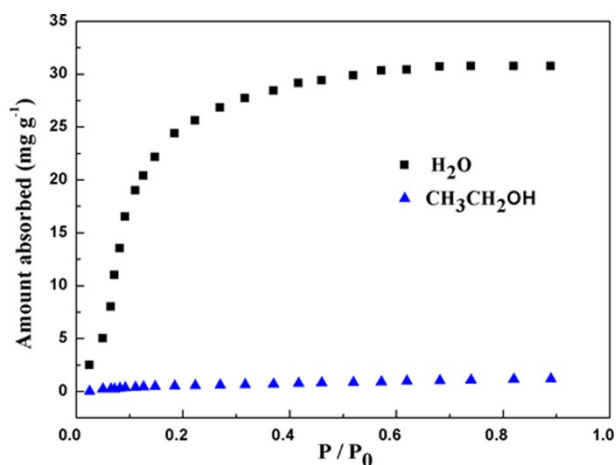


Fig. 3. Water (■) and ethanol (▲) adsorption isotherms of **1** at 298 K.

#### Anion-exchange properties

The crystals of **1** have excellent stability for months under air atmosphere or immersing them in water, and no efflorescence was observed. The stability of **1** was also confirmed by PXRD analysis (Fig. S2). Meanwhile, **1** is a rare cationic framework, where OH<sup>-</sup> anions are located. As a result of the compositional features, we speculated that encapsulated OH<sup>-</sup> anions could be replaced by other small inorganic anions. As we know, thiocyanate (SCN<sup>-</sup>) is a toxic anionic pollutant, occurring from electroplating, dyeing and other industries.<sup>27</sup> The SCN<sup>-</sup> can adversely affect human health by impairing thyroid and renal function. Thus, we performed the SCN<sup>-</sup> removal via anion exchange under ambient conditions. The crystals sample of **1** (100.12 mg) were weighed accurately and then immersed into a aqueous solutions (0.20 M, 30 mL) of KSCN for 48 h, the exchanged sample was filtered and further washed several times with deionized water and dried in air. The final anion-exchanged products were identified by IR spectrum, PXRD and element analysis. In the IR spectrum of the exchanged sample, a new strong band at 2082 cm<sup>-1</sup> appears compared with the as-synthesized sample (Fig. S3), which corresponds to the characteristic adsorption band of SCN<sup>-</sup>.<sup>28</sup> Meanwhile, the slight shifts of the other bands in the exchanged sample are owing to the exchange process. These changes also suggest that the OH<sup>-</sup> anions in **1** were exchanged by SCN<sup>-</sup> anions. Furthermore, the PXRD pattern of the exchanged sample exhibited the crystalline state of **1** was retained (Fig. S2). The final mass of exchanged products was 101.38 mg (increased by 1.26 wt%, elemental analysis: S, 1.02 wt%). Based on the mass change and element analysis, around 90% OH<sup>-</sup> of **1** was replaced by SCN<sup>-</sup> during the exchange process.

#### Conclusions

In summary, an arsenicniobate-based porous framework has been synthesized under hydrothermal conditions. And, a tetra-vanadyl capped arsenicniobate {AsNb<sub>12</sub>V<sub>4</sub>} cluster is firstly constructed here. The successful synthesis of compound **1** prove again the effectivity of hydrothermal techniques in designing Nb/V hybrid heteropolyoxoniobates. Adsorption properties show that **1** can selectively adsorb water molecules over ethanol to make azeotrope separate. Besides, anion-exchange studies suggest that **1** can efficiently remove toxic SCN<sup>-</sup> anions in aqueous solution.

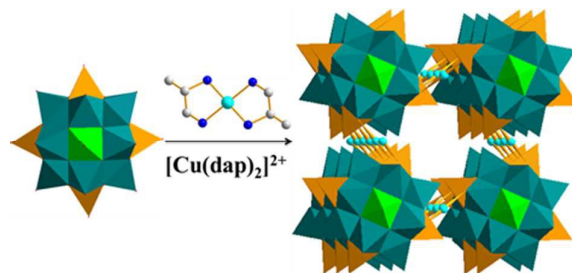
#### Acknowledgements

This work was supported by the National Natural Science Foundation of China (Grants 21171032, 21371029, 21231002 and 21571030), the Key Technologies R&D Program of Jilin Province of China (Grant 201302060795F), and the Open Research Fund of the State Key Laboratory of Inorganic Synthesis and Preparative Chemistry (Jilin University, Grant 2015-01).

#### Notes and references

- (a) M. Sun, J. Zhang, P. Putaj, V. Caps, F. Lefebvre, J. Pelletier and J. M. Basset, *Chem. Rev.*, 2014, **114**, 981–1019; (b) A. P. Griset, J. Walpole, R. Liu, A. Gaffey, Y. L. Colson and M. W. Grinstaff, *J. Am. Chem. Soc.*, 2009, **131**, 2469–2471; (c) A. Müller, F. Peters, M. T. Pope and D. Gatteschi, *Chem. Rev.*, 1998, **98**, 239–271.
- (a) F. J. Ma, S. X. Liu, C. Y. Sun, D. D. Liang, G. J. Ren, F. Wei, Y. G. Chen and Z. M. Su, *J. Am. Chem. Soc.*, 2011, **133**, 4178–4181; (b) C. J. Jiang, A. Lesbani, R. Kawamoto and N. Mizuno, *Am. Chem. Soc.*, 2006, **128**, 14240–14241; (c) C. Lydon, C. Busche, H. N. Miras, A. Delf, D. L. Long, L. Yellowlees and L. Cronin, *Angew. Chem., Int. Ed.*, 2012, **51**, 2115–2118; (d) L. Wang, B. B. Zhou, K. Yu, Z. H. Su, S. Gao, L. L. Chu, J. R. Liu and G. Y. Yang, *Inorg. Chem.*, 2013, **52**, 5119–5127.
- (a) X. L. Wang, Y. F. Bi, B. K. Chen, H. Y. Lin and G. H. Liu, *Inorg. Chem.*, 2008, **47**, 2442–2448; (b) X. L. Wang, H. L. Hu, A. X. Tian and H. Y. Lin, *Inorg. Chem.*, 2010, **49**, 10299–10306; (c) B. S. Bassil, M. Ibrahim, M. Asano, Z. X. Wang, N. S. Dalal, N. N. Biboum, B. Keita, L. Nadjjo and U. Körtz, *Angew. Chem. Int. Ed.*, 2011, **50**, 5961–5964; (d) J. Yan, D. L. Long and L. Cronin, *Angew. Chem. Int. Ed.*, 2010, **49**, 4117–4120; (e) A. RuizdelOliva, V. Sans, H. N. Miras, H. Y. Zang, D. L. Long and L. Cronin, *Angew. Chem. Int. Ed.*, 2012, **51**, 12759–12762.
- (a) Z. Zhou, J. P. Wang and J. Y. Niu, *Inorg. Chem.*, 2013, **52**, 8285–8287; (b) R. Mekala, S. Supriya and S. K. Das, *Inorg. Chem.*, 2013, **52**, 9708–9710; (c) A. Banerjee, N. Vankova, B. S. Bassil, T. Heine and U. Körtz, *Inorg. Chem.*, 2011, **50**, 11667–11675; (d) X. K. Fang, L. Hansen, F. Haso, P. C. Yin, A. Pandey, L. Engelhardt, I. Slowing, T. Li, T. B. Liu and D. C. Johnston, *Angew. Chem.*, 2013, **125**, 10694–10698; (e) J. M. Breen and W. Schmitt, *Angew. Chem. Int. Ed.*, 2008, **47**, 6904–6908.
- (a) I. Lindqvist and Ark. Kemi 1952, **5**, 247; (b) E. J. Graeber and B. Morosin, *Acta Crystallogr. Sect. B*, 1977, **33**, 2137–2143; (c) M. Filowitz, W. G. Klempner and W. Shum, *Inorg. Chem.*, 1979, **18**, 93–103; (d) M. Maekawa, Y. Ozawa and A. Yagasaki, *Inorg. Chem.*, 2006, **45**, 9608–9609; (e) R. P.

- Bontchev and M. Nyman, *Angew. Chem., Int. Ed.*, 2006, **45**, 6670–6672.
- 6 (a) R. Tsunashima, D. L. Long, H. N. Miras, D. Gabb, C. P. Pradeep and L. Cronin, *Angew. Chem. Int. Ed.*, 2010, **49**, 113–116; (b) P. Huang, C. Qin, Z. M. Su, Y. Xing, X. L. Wang, K. Z. Shao, Y. Q. Lan and E. B. Wang, *J. Am. Chem. Soc.*, 2012, **134**, 14004–14010.
- 7 (a) J. Y. Niu, G. Chen, J. W. Zhao, P. T. Ma, S. Z. Li, J. P. Wang, M. X. Bai, Y. Li and B. S. Ji, *Chem.–Eur. J.*, 2010, **16**, 7082–7086; (b) J. Y. Niu, P. T. Ma, H. Y. Niu, J. Li, J. W. Zhao, Y. Song and J. P. Wang, *Chem.–Eur. J.*, 2007, **13**, 8739–8748; (c) J. Y. Niu, F. Li, J. W. Zhao, P. T. Ma, D. D. Zhang and J. P. Wang, *Chem.–Eur. J.*, 2014, **20**, 9852–9857; (d) J. H. Son, C. A. Ohlin and W. H. Casey, *Dalton Trans.*, 2012, **41**, 12674–12677.
- 8 (a) C. A. Ohlin, E. M. Villa, J. C. Fettinger and W. H. Casey, *Dalton Trans.*, 2009, **15**, 2677–2678; (b) M. Nyman, L. J. Criscenti, F. Bonhomme, M. A. Rodriguez and R. T. Cygan, *J. Solid State Chem.*, 2003, **176**, 111–119; (c) C. A. Ohlin, E. M. Villa, J. C. Fettinger and W. H. Casey, *Angew. Chem. Int. Ed.*, 2008, **47**, 5634–5636; (d) J. H. Son, C. A. Ohlin and W. H. Casey, *Dalton Trans.*, 2013, **42**, 7529–7533.
- 9 (a) G. L. Guo, Y. Q. Xu, J. Cao and C. W. Hu, *Chem.–Eur. J.*, 2012, **18**, 3493–3497; (b) Z. J. Liang, D. D. Zhang, P. T. Ma and J. Y. Niu, *Chem.–Eur. J.*, 2015, **21**, 1–5; (c) P. Huang, C. Qin, X. L. Wang, C. Y. Sun, G. S. Yang, K. Z. Shao, Y. Q. Jiao, K. Zhou and Z. M. Su, *Chem. Commun.*, 2012, **48**, 103–105.
- 10 M. Nyman, F. Bonhomme, T. M. Alam, M. A. Rodriguez, B. R. Cherry, J. L. Krumhansl, T. M. Nenoff and A. M. Sattler, *Science*, 2002, **297**, 996–998.
- 11 M. Nyman, F. Bonhomme, T. M. Alam, J. B. Parise and G. M. B. Vaughan, *Angew. Chem., Int. Ed.*, 2004, **43**, 2787–2792.
- 12 (a) F. Bonhomme, J. P. Larentzos, T. M. Alam, E. J. Maginn and M. Nyman, *Inorg. Chem.*, 2005, **44**, 1774–1785; (b) Z. Zhang, Q. Lin, D. Kurunthu, T. Wu, F. Zuo, S. T. Zheng, C. J. Bardeen, X. Bu and P. Feng, *J. Am. Chem. Soc.*, 2011, **133**, 6934–6937.
- 13 (a) X. Zhang, S. X. Liu, Y. H. Gao and X. N. Wang, *Eur. J. Inorg. Chem.*, 2013, 1706–1712; (b) T. M. Anderson, T. M. Alam, M. A. Rodriguez, J. N. Bixler and M. Nyman, *Inorg. Chem.*, 2008, **47**, 7834–7839.
- 14 (a) Y. Hou, M. Nyman and M. A. Rodriguez, *Angew. Chem. Int. Ed.*, 2011, **50**, 12514–12517; (b) Y. Hou, T. M. Alam, M. A. Rodriguez and M. Nyman, *Chem. Commun.*, 2012, **48**, 6004–6006.
- 15 Y. Hou, L. N. Zakharov and M. Nyman, *J. Am. Chem. Soc.*, 2013, **135**, 16651–16657.
- 16 (a) J. H. Son, C. A. Ohlin, E. C. Larson, P. Yu and W. H. Casey, *Eur. J. Inorg. Chem.*, 2013, 1748–1753; (b) G. Guo, Y. Xu, J. Cao and C. W. Hu, *Chem. Commun.*, 2011, **47**, 9411–9413; (c) J. H. Son, C. A. Ohlin, R. L. Johnson, P. Yu and W. H. Casey, *Chem.–Eur. J.*, 2013, **19**, 5191–5197; (d) Y. Zhang, J. Q. Shen, L. H. Zheng, Z. M. Zhang, Y. X. Li and E. B. Wang, *Cryst. Growth Des.*, 2014, **14**, 110–116.
- 17 J. Q. Shen, Q. Wu, Y. Zhang, Z. M. Zhang, Y. G. Li, Y. Lu and E. B. Wang, *Chem.–Eur. J.*, 2014, **20**, 2840–2848.
- 18 J. Q. Shen, Y. Zhang, Z. M. Zhang, Y. G. Li and E. B. Wang, *Chem. Commun.*, 2014, **50**, 6017–6019.
- 19 P. Huang, E. L. Zhou, X. L. Wang, C. Y. Sun, Y. Xing, K. Z. Shao and Z. M. Su, *CrystEngComm.*, 2014, **16**, 9582–9585.
- 20 (a) Z. Y. Zhang, J. Peng, Z. Y. Shi, W. L. Zhou, S. U. Khana and H. S. Liu, *Chem. Commun.*, 2015, **51**, 3091–3093; (b) Q. Lan, Z. M. Zhang, Y. G. Li and E. B. Wang, *RSC Adv.*, 2015, **5**, 44198–44203.
- 21 S. J. Li, S. X. Liu, C. C. Li, F. J. Ma, W. Zhang, D. D. Liang, R. K. Tan, Y. Y. Zhang and Q. Tang, *Inorg. Chim. Acta*, 2011, **376**, 296–301.
- 22 (a) M. Filowitz, R. K. C. Ho, W. G. Klemperer and W. Shum, *Inorg. Chem.*, 1979, **18**, 93–103; (b) F. J. Farrell, V. A. Maroni and T. G. Spiro, *Inorg. Chem.*, 1969, **8**, 2638–2642; (c) C. M. Flynn and G. D. Stucky, *Inorg. Chem.*, 1969, **8**, 178–180.
- 23 N. F. M. Henry, K. Lonsdale (Eds.) *International Tables for X-ray Crystallography* Kynoch Press: Birmingham, U. K. 1952.
- 24 G. M. Sheldrick, *SHELXS-97, Program for the Refinement of Crystal Structure* University of Göttingen: Göttingen, Germany, 1997.
- 25 A. L. Spek, *PLATON 99: A Multipurpose Crystallographic Tool* Utrecht University: Utrecht, The Netherlands, 1999.
- 26 C. R. Deltcheff, M. Fournier, R. Franck and R. Thouvenot, *Inorg. Chem.*, 1983, **22**, 207–216.
- 27 S. Hou, Q. k. Liu, J. P. Ma and Y. B. Dong, *Inorg. Chem.*, 2013, **52**, 3225–3235.
- 28 (a) L. H. Xie, S. X. Liu, C. Y. Gao, R. G. Cao and J. F. Cao, *Inorg. Chem.*, 2007, **46**, 7782–7788; (b) Q. R. Fang, G. S. Zhu, M. Xue, J. Y. Sun, Y. Wei, S. L. Qiu and R. R. Xu, *Angew. Chem., Int. Ed.*, 2005, **44**, 3845–3848; (c) Y. Q. Chen, G. R. Li, Z. Chang, Y. K. Qu and X. H. Bu, *Chem. Sci.*, 2013, **4**, 3678–3682.

**Table of contents:**

An arsenicniobate-based cationic framework shows high adsorption selectivity of water and ethanol and effective removal of toxic  $\text{SCN}^-$  anions.